Radiative Capture of s Electrons in the Decay of ^{51}Cr†

Manfred Mutterer*
Central Bureau for Nuclear Measurements, EURATOM, 2440 Geel, Belgium
(Received 19 December 1972)

The high-energy portion of the spectrum of internal-bremsstrahlung photons accompanying the allowed electron-capture transition from ^{51}Cr to the ground state of ^{51}V has been measured with a Ge(Li) γ-ray spectrometer supplied with a pileup rejector. The most important correction for the residual pileup spectrum caused by the 320.1-keV nuclear γ rays from the deexcitation of the first excited state in ^{51}V was performed by extrapolation from a set of measurements with sources of different activities. The pulse-height spectrum of internal-bremsstrahlung photons was corrected for detector response. For energies higher than 348.1 keV the number of bremsstrahlung photons emitted per ground-state electron-capture (EC) decay of ^{51}Cr was determined to be $(9.56 \pm 0.60) \times 10^{-5}$. Corresponding theoretical values are 9.49×10^{-5} predicted by the theory of Martin and Glauber, and 9.47×10^{-5} deduced from recent calculations of Intemann. The present result confirms the predictions of theory for radiative capture of $1s + 2s$ orbital electrons, in contradiction to recent results on ^{51}Cr and other EC decaying light nuclides, obtained mainly by bremsstrahlung-γ-coincidence measurements. The transition energy of ^{51}Cr was determined to be 760 ± 15 keV, in good agreement with accepted atomic mass differences.

1. INTRODUCTION

In nuclear decay by electron capture (EC) a small fraction (usually $\sim 10^{-4}$) of the decay events is accompanied by internal bremsstrahlung (IB). The study of this radiative capture process provides a lot of information on EC decay, and many investigations, both theoretical[1-9] and experimental,[10-12] have been devoted to it.

The IB theory for allowed EC decays has been most extensively developed by Martin and Glauber,[2,3] who improved the early theory of Morrison and Schiff[1] by taking account of the nuclear Coulomb field and of relativistic and screening effects. Their calculations include also capture of electrons from higher shells. It is well known from this work that IB associated with capture of s-orbital electrons is dominant for photon energies higher than about $Z\alpha$ (units of mc^2; Z is the atomic number; α is the fine-structure constant), while IB due to p-electron capture is considerably intense at lower energies. This theory, which includes some low-Z approximations, was supplemented very recently by more accurate numerical calculations.[5,6]

The agreement between theory and experiments is not yet satisfactory. Although experiments in general confirm the predicted shape of an allowed IB spectrum the results for the absolute number of photons per disintegration are still rather controversial. For s IB in low-Z EC transitions, where the calculations are most accurate, ratios of experimental to theoretical intensities between 0.5 and 1.5 are found, even if best available values for the transition energies[13] are used to calculate the theoretical quantities.[11,14] A number of experiments have been published recently,[14-17] in which IB spectra have been separated from spectra of much more intense nuclear γ rays by measuring IB-γ coincidences. In part of these measurements[15] the intensity of IB was found to be 20 to 40% lower than the predictions of theory; others[14,16,17] have yielded 20 to 30% higher results than theory. In one recent experiment[18] the intensity of circularly polarized IB in the ^{51}Cr decay has been measured with a Compton polarimeter to be (67 ± 7)% of the predicted intensity. The large inconsistency mainly among the IB-γ-coincidence results has prompted the present investigation.

A relative measurement of IB to γ intensity is possible for nuclides that decay by competing EC branches to the ground state and to excited states in the daughter nuclei, respectively. Here part of the IB accompanying the ground-state branch falls always into the energy region above the nuclear-γ-ray energy. The measurement of the IB in this region with a γ-ray spectrometer is, however, strongly complicated by pileup from the γ-ray pulses being more frequent by several orders of magnitude.

The decays of ^{51}Cr and 'Be are favorable for such an IB/γ measurement. In both cases, a large fraction of the IB spectrum exceeds the γ energy, and γ emission occurs only in about 10% of the decays, reducing pileup contributions to a treatable amount. The use of a high-resolution Ge(Li) γ-ray spectrometer further facilitates the separation of IB and pileup.

The γ branching ratios in both decays are accurately known, so that good results on the rela-

tive rate of radiative to ordinary capture for the predominant ground-state branches can be derived from measured IB/γ ratios. The predictions for this rate from IB theory can accurately be calculated, since precise values for the transition energies are available. The accurate determination of the IB intensities, on the other hand, will provide good IB corrections for accurate γ calibration of both nuclides.

In the present paper our measurements on ^{51}Cr are described; the results on ^{7}Be will be contained in a subsequent paper.[19]

2. EXPERIMENTS

A. Experimental Technique

A Ge(Li) detector with a volume of 1.2 cm^3 (diameter, 14 mm; thickness, 8 mm) was used, in conjunction with a TMC 336 preamplifier, an ESONE A 1005 nonoverloading linear amplifier, and a SCIPP-1600 pulse-height analyzer operated with conversion gain 800. The energy calibration was performed by recording spectra from standard sources of ^{139}Ce (165.8 keV), ^{51}Cr (320.1 keV), ^{7}Be (477.6 keV), ^{85}Sr (514.0 keV), ^{137}Cs (661.6 keV), ^{95}Nb (765.8 keV), ^{54}Mn (835.0 keV), and ^{65}Zn (1115.4 keV), and determining the photopeak positions by the three-channel method.[20]

For the ^{51}Cr measurements an electronic pulse pileup rejection system was used (Fig. 1), the principal element of which is a pileup gate (EGG-GP 100/N) coupled to the anticoincidence gate of the analyzer. Pileup rejection was performed for pulse intervals between the resolving time τ_{min} and 3.6 μsec and for pulses higher than 5% of the amplitude of the 320.1-keV γ pulses. The resolving time was about 100 nsec for two pulses of equal amplitude and varied between about 50 and 200 nsec for pulses of different heights.

This procedure reduced pileup considerably (by a factor of 10 for an integration and differentiation time constant of 0.5 μsec in the main amplifier), but the residual pileup spectrum formed by pulses

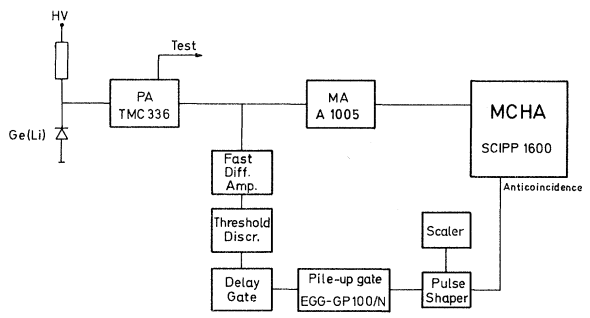

FIG. 1. Block diagram of the electronic equipment of the Ge(Li) γ-ray spectrometer with pileup rejection.

of the nuclear γ rays could not be reduced to an amount negligible compared to the weak IB spectrum. This was even true for total counting rates as low as 10^3 sec^{-1}, where the IB counting rate above the nuclear-γ-ray energy became comparable to the rate of the natural background radiation. A previous attempt[21] to measure the IB spectrum of ^{51}Cr with a similar arrangement was unsuccessful for this reason.

The complete separation of the residual pileup and IB spectrum, however, can be attained by measuring sources of different activities and extracting the pure IB contribution from an extrapolation procedure to zero activity.

B. Extrapolation Method

In each measured spectrum the counting rate $n_{ap}(E, N)$ in every channel (corresponding to an energy range $E-\frac{1}{2}\Delta E \leq E < E+\frac{1}{2}\Delta E$) above the photopeak energy is the sum of counts from residual pileup $n'_{pu}(E, N')$, internal bremsstrahlung

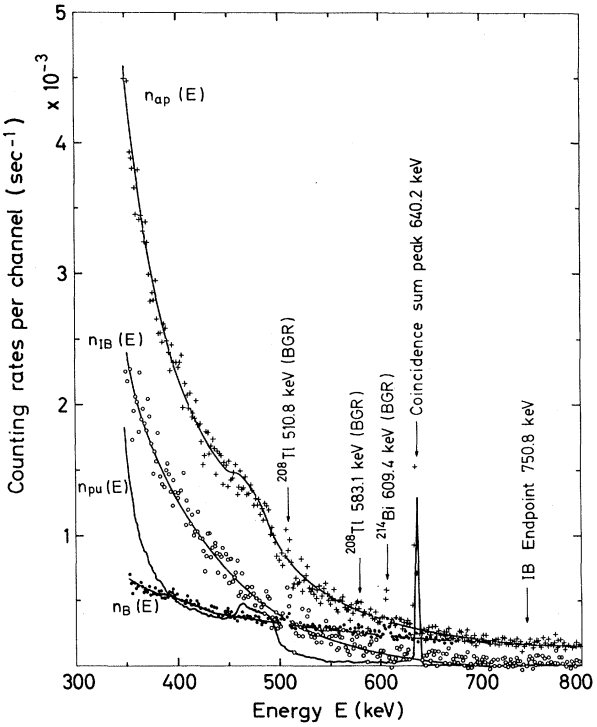

FIG. 2. Photon spectrum $n_{ap}(E)$ in the energy range 348.1 keV $\leq E \leq$ 800 keV of a weak ^{51}Cr source (disintegration rate: 7×10^5 sec^{-1}) as recorded for 5100 min with a 1.2-cm^3 Ge(Li) γ-ray spectrometer supplied with a pileup rejector. The individual contributions of internal-bremsstrahlung photons $n_{IB}(E)$, and residual pileup pulses $n_{pu}(E)$ from the 320.1-keV nuclear γ rays were determined in combination with a spectrum of a strong source (9×10^6 sec^{-1}). The background spectrum $n_B(E)$ was measured for 11 900 min.

$n'_{IB}(E, N')$, and background $n'_B(E)$ (see, e.g., Fig. 2), multiplied by a correction function $f(N)$ for over-all rejection losses:

$$n_{ap}(E, N) = [n'_{pu}(E, N') + n'_{IB}(E, N') + n'_B(E)] f(N). \quad (2.1)$$

The correction function $f(N)$ is given by $f(N) = N/N'$, where N is the total counting rate integrated over the whole γ spectrum, and N' is the rate of events recorded by the detector. Since nearly all counts ($\gtrsim 99.7\%$) in the total spectrum are due to the nuclear γ rays, the function $f(N)$ can easily be determined by comparing the counting rates N with the known γ-emission rates of the used sources.

After subtraction of the background term $n'_B(E)f(N)$ from $n_{ap}(E, N)$ and introduction of the N'-independent ratios

$$s_{pu}(E) = n'_{pu}(E, N')/N'^2$$

and

$$r_{IB}(E) = n'_{IB}(E, N')/N'$$

one gets

$$n(E, N)/N = s_{pu}(E)N' + r_{IB}(E). \quad (2.2)$$

For counting rates lower than 2×10^4 sec^{-1} as used in our experiment, the quantity $\tau_{min}N'$ is always much smaller ($\leq 4\times10^{-3}$) than unity and, consequently, the pileup shape function $s_{pu}(E)$ is in good approximation determined by first-order pileup only. In the idealized case of rectangular pulses and constant resolving time τ_{min}, the function $s_{pu}(E)$ for first-order pileup is independent of N', as claimed in Eq. (2.2):

$$s_{pu}(E) = \tau_{min}(N')^{-2} \times \int_{E-(1/2)\Delta E}^{E+(1/2)\Delta E} dE' \int_0^{E'} dx\, n_\gamma(E'-x, N') \times n_\gamma(x, N'). \quad (2.3)$$

The shape of the measured residual pileup spectrum (Fig. 2) comes close to that idealized shape, since τ_{min} is short compared to that flat maximum of the main amplifier pulses. A distinct difference is observed only in the low-energy part ($E_\gamma < E \lesssim 450$ keV), where the observed spectrum rises more steeply. This can be explained by the variation of τ_{min} with the pulse amplitudes, and the independence of $s_{pu}(E)$ on N' can be assumed to be conserved.

In this case, the pure IB spectrum $r_{IB}(E)$ per recorded γ event can be determined from a set of measured spectra by linearly extrapolating the quantities $n(E, N)/N$ as function of N' to $N' \to 0$. In order to check this assumption we made also extrapolations of integral counting rates in the energy region above the photopeak, according to

$$N_{int}/N = S_{pu}N' + R_{IB}, \quad (2.4)$$

with the definitions

$$N_{int} = \sum_{E_1}^{E_2} n(E, N), \quad S_{pu} = \sum_{E_1}^{E_2} s_{pu}(E),$$

and

$$R_{IB} = \sum_{E_1}^{E_2} r_{IB}(E),$$

and conditions for the integration limits

$$E_1 > E_\gamma \quad \text{and} \quad E_2 > E^{IB}_{max}.$$

C. Experimental Details and Determination of the IB Spectrum

All sources, used for the IB measurements and for the calibration of the device (Sec. 3 B), were drop sources deposited and dried onto small polyethylene foils. Care has been taken that the activity was distributed over a circularly shaped area of 4 ± 1 mm diam. The foils were then fixed and sealed into aluminum containers which were placed at a reproducible position located 10 mm distant from the detector surface.

The counting geometry of all sources used was equal within 1.5% under the given conditions. The γ-emission rates of the sources have been determined with an accuracy of 0.5 to 1% by integral counting with a calibrated NaI(Tl) γ-ray spectrometer.[22]

The ^{51}Cr sources were prepared from a carrier-free $^{51}CrCl_3$ solution, which before had been radiochemically purified by extracting the impurities with TIOA (triisooctylamine) (10% volume) -xylene (90% volume).[23] No impurity peaks could be detected in the energy range below 2 MeV; for energies higher than 350 keV the limit of detection was $<10^{-7}$ in respect to the ^{51}Cr γ activity.

To determine the IB spectrum of ^{51}Cr a total number of 10 spectra has been recorded using 6 sources. The time of the single measurements ranged from 700 min for the strongest source (^{51}Cr activity of 9×10^6 sec^{-1}) to 5100 min for the weakest one (7×10^5 sec^{-1}). Eight background spectra were recorded during the whole period of measurements for a total 11 900 min. The intensity of the background radiation was found to be stable within the statistical errors of $\leq 2\%$ on the integral background rates in the energy range of the measured IB spectrum. The mean of all background spectra was subtracted from the ^{51}Cr spectra after multiplication with the function $f(N)$. This correction function for over-all rejection

losses could be determined from the series of measurements on ^{51}Cr and ^{7}Be[19] to be $f(N)=1-aN$, with $a=7.05\pm0.20$ μsec.

For the extrapolation of integral counting rates N_{int} according to Eq. (2.4), an upper integration limit E_2 of 810 keV and several lower limits E_1 between 332.1 and 396.0 keV were chosen. Straight lines were fitted to the data (Fig. 3) using two different least-squares-fitting procedures, one without weighting the individual points (fit I) and a second using the squared reciprocals of the statistical errors on both axes (generally $\lesssim 1\%$) as weights[24] (fit II), respectively. The results of both fits agree satisfactorily: For example, for $E_1=348.1$ keV (curve b in Fig. 3) the slopes determined by both fits differ by less than 0.4%, the calculated standard errors being 0.3 and 0.9%, respectively. The intercept R_{IB}, corresponding to the total number of IB quanta recorded in the energy range $E\geq 348.1$ keV per recorded γ quantum, was calculated to be $R_{\text{IB}}=(1.068\pm0.014)\times10^{-4}$. The results from both fits differed, in this case, less than 1% from calculated standard errors of 1.2 and 1.4%, respectively. The resulting small errors support the assumed proportionality of the integral pileup rates with N' [Eq. (2.4)].

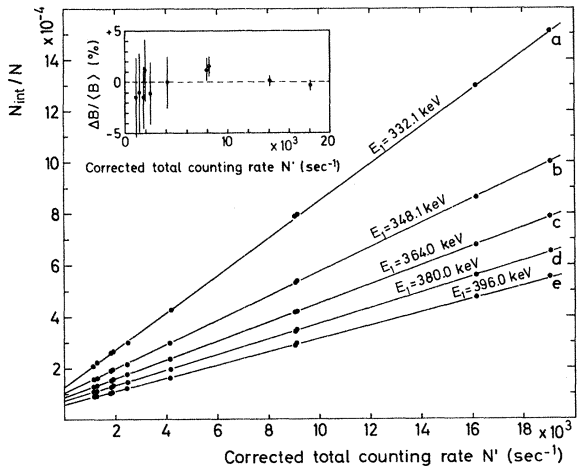

FIG. 3. Ratios of integral counting rates N_{int} within energy intervals $E_1\leq E\leq 810$ keV and total counting rates N (0 to 810 keV) versus the total counting rates N' that have been corrected for over-all rejection losses. Curves a to e were obtained by least-squares fitting of straight lines to the results of 10 measurements using several lower-energy limits E_1 [Eq. (2.4)]. The experimental errors are within the diameters of the plotted points. The extrapolations to $N\to 0$ yield integral rates $R_{\text{IB}}(E_1)$ of IB photons per recorded nuclear γ quantum of ^{51}Cr. The inset shows the calculated deviations $\Delta B=B-\langle B\rangle$ of the ratios $B=S_{\text{pu}}(E_1=332.1\text{ keV})/S_{\text{pu}}(E_1=396.0\text{ keV})$ of integral pileup counting rates from the mean value $\langle B\rangle=2.80$.

As a sensitive check of the constancy of $s_{\text{pu}}(E)$ in the energy range of strongest deviation from the idealized shape [Eq. (2.3)], pileup rates $S_{\text{pu}}(E_1)N'$ were calculated by subtracting the extrapolated values $R_{\text{IB}}(E_1)$ from the quantities $N_{\text{int}}(E_1)/N$, and the ratio $B\equiv S_{\text{pu}}(E_1=332.1\text{ keV})/S_{\text{pu}}(E_1=396.0\text{ keV})$ was regarded as function of N'. The inset in Fig. 3 shows the deviations $\Delta B=B-\langle B\rangle$ from the mean value $\langle B\rangle=2.80$, which were, at maximum, 1.5% of $\langle B\rangle$ and within the statistical errors. This justifies a linear extrapolation procedure in the covered energy range.

The differential IB spectrum per total count rate, $r_{\text{IB}}(E)$, was determined by weighted least-squares fitting of straight lines to the rates $n(E,N)/N$ in every channel [Eq. (2.2)]. The final experimental IB spectrum $n_{\text{IB}}^{\text{exp}}(E)$ per energy interval of 1 keV and per ground-state EC decay of ^{51}Cr (Fig. 4) was then calculated from $r_{\text{IB}}(E)$ according to

$$n_{\text{IB}}^{\text{exp}}(E)=r_{\text{IB}}(E)P_\gamma\epsilon_\gamma^0/(1-P_\gamma)\Delta E. \tag{2.5}$$

In Eq. (2.5) $P_\gamma=0.098\pm0.002$[25] is the branching ratio in the ^{51}Cr decay, and $\Delta E=1.597\pm0.003$ keV is the energy interval per channel width of our analyzer setting. The total counting efficiency for the nuclear γ rays, $\epsilon_\gamma^0=N'/A_\gamma=(1.907\pm0.035)\times10^{-2}$, was determined as a mean from the corrected total count rates N' and the known γ-emission rates A_γ of the used sources.

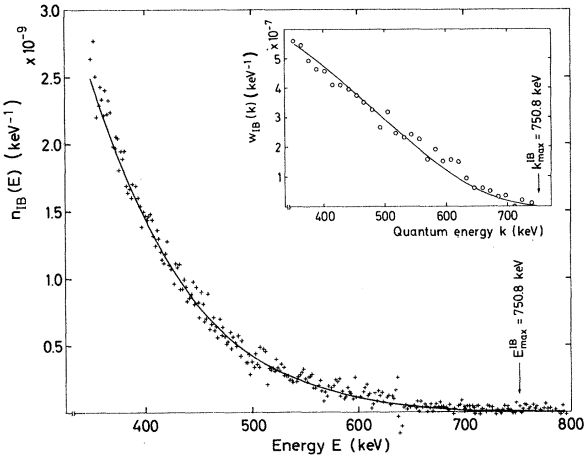

FIG. 4. Pulse-height spectrum $n_{\text{IB}}(E)$ of ^{51}Cr internal-bremsstrahlung photons. The experimental spectrum $n_{\text{IB}}^{\text{exp}}(E)$ was determined by weighted least-squares fitting of straight lines to the measured rates $n(E,N)/N$ versus N' [Eq. (2.2)] and was normalized according to Eq. (2.5). The full line is the IB pulse-height spectrum $n_{\text{IB}}^{\text{th}}(E)$, that was calculated from the Martin-Glauber theory using $Q_{\text{EC}}=751.4$ keV and folded with the response function of the γ-ray spectrometer. The inset shows the theoretical IB spectrum $w_{\text{IB}}^{\text{th}}(k)$ and the response-corrected experimental spectrum $w_{\text{IB}}^{\text{exp}}(k)$.

3. COMPARISON WITH THEORY

A. Theoretical Spectrum

For the low-Z isotope ^{51}Cr internal bremsstrahlung accompanying capture of p-orbital electrons is negligibly small for photon energies much higher than about 90 keV ($\approx Z\alpha$), as in the energy range covered by our experiment. The comparison with theory can therefore be restricted to radiative capture of s electrons only, the predominant contribution ($\gtrsim 99\%$) of which pertains to $1s$ and $2s$ capture. Thus for each branch in the ^{51}Cr decay the IB spectrum $w_{\mathrm{IB}}^{\mathrm{th}}(k)dk$ per EC decay can be calculated from the theory of Martin and Glauber[2,3] according to

$$w_{\mathrm{IB}}^{\mathrm{th}}(k)dk = (\alpha/\pi)k\,dk\left[P_K(1-k/k_{\max}^{1s})^2 R_{1s}(Z,k) + P_{L_1}(1-k/k_{\max}^{2s})^2 R_{2s}(Z,k)\right]. \tag{3.1}$$

In Eq. (3.1) the quantity α is the fine-structure constant, k is the photon energy in units of the electron rest mass, P_K and P_{L_1} are the relative capture probabilities for electrons from the $1s$ and $2s$ shell, respectively, the $R_{ns}(Z,k)$ are the shape factors, and the $k_{\max}^{ns}$ are the end-point energies of the partial ns-IB spectra. The latter are given by the transition energy Q_{EC} minus the binding energy k_{B}^{ns} of the captured ns electrons.

In our calculation we used for Q_{EC} a value of 751.4 ± 0.9 keV from the most recent atomic-mass tables.[13] Values for P_K, P_{L_1}, and the binding energies k_{B}^{1s} and k_{B}^{2s} have been derived from literature.[26-29] The shape factors $R_{1s}(Z,k)$ and $R_{2s}(Z,k)$ were calculated from the theory of Martin and Glauber [Eqs. (4.3) and (4.4) in Ref. 3, and Eqs. (9.16) and (9.25) in Ref. 2, respectively], and from improved calculations on the basis of this theory, presented recently by Intemann.[6] The IB accompanying the EC branch to the excited level of ^{51}V ($Q_{\mathrm{EC}}^{*} = 431.3 \pm 1.0$ keV) turns out to contribute only 0.2% to the total IB intensity for $k \geq 348.1$ keV and has therefore been neglected.

Equation (3.1) can be written in another form by introducing $w_{\mathrm{IB}}^{\mathrm{CF}}(k, k_{\max}^{1s})$, the result of the earlier "Coulomb-free" approach of Morrison and Schiff,[1] which contains the major dependence on the photon energy k:

$$w_{\mathrm{IB}}^{\mathrm{th}}(k)dk = R_s(Z,k)\,w_{\mathrm{IB}}^{\mathrm{CF}}(k, k_{\max}^{1s})dk, \tag{3.2}$$

$$w_{\mathrm{IB}}^{\mathrm{CF}}(k, k_{\max}^{1s})dk = (\alpha/\pi)k(1-k/k_{\max}^{1s})^2 dk. \tag{3.3}$$

The function $R_s(Z,k)$, which can be defined as an over-all shape function for s-IB radiation, is only slightly varying with k but dominantly dependent on the atomic number Z:

$$R_s(Z,k) = P_K R_{1s}(Z,k) + P_{L_1} R_{2s}(Z,k)h(k). \tag{3.4}$$

The function $h(k)$ introduced in Eq. (3.4) corrects for the difference in binding energy of the $1s$ and $2s$ electrons ($k_{\mathrm{B}}^{1s} - k_{\mathrm{B}}^{2s} = 5.3$ keV $\approx k_{KX}$) and has a strong influence near the end point of the IB spectrum:

$$h(k) = (1-k/k_{\max}^{2s})^2/(1-k/k_{\max}^{1s})^2 \approx \left[1 + k_{KX}/(k_{\max}^{1s} - k)\right]^2. \tag{3.5}$$

The description of the total s-IB spectrum by Eqs. (3.2) to (3.5) will be used to determine the $1s$-IB end-point energy by applying a Jauch plot to the measured IB spectrum (Sec. 3 C).

B. Correction for Detector Response

The energy spectrum $w_j = w(k_j)$ of photons emitted by the source and the pulse-height spectrum $n_i = n(E_i)$ recorded in m channels of the analyzer are linked by the set of equations:

$$\sum_{j=1}^{m} r_{ij}\,w_j = n_i \quad (i = 1, \ldots, m). \tag{3.6}$$

The coefficients $r_{ij} = r(E_i, k_j)$ compose the so-called response matrix R, which for the comparison of the theoretical and experimental IB spectrum must be known with sufficient accuracy.

The columns of R are represented by pulse-height spectra measured per unit time with monoenergetic γ sources of energies k_j and unit decay rates. Thus, spectra of calibrated γ sources (^{51}Cr, ^{7}Be, ^{85}Sr, ^{137}Cs, ^{95}Nb, ^{54}Mn, and ^{65}Zn) were recorded and divided by the known γ-emission rates. The matrix elements r_{ij} in the energy range from 320 keV to 1 MeV were determined by interpolation. Favorably, two different interpolation procedures were used for the photopeaks and the remaining parts of the spectra including the Compton distributions, respectively:

(a) The photopeak efficiency $\epsilon_p(k)$ and energy resolution $\Delta E(k)$ of the device were determined from spectra of the peak regions, recorded by using a biased amplifier. Second-order polynomials in k were fitted to the sets of data ΔE versus k and $\log\epsilon_p$ versus $\log k$, respectively. From these functions the elements of R near the diagonal have been calculated as histograms of normalized Gaussian peaks.

(b) To get the remaining part of R, the calibration spectra were transformed to a new energy scale ϵ bringing all Compton edges in the transformed spectra $\tilde{n}(\epsilon, k)$ to the same position at $\epsilon = 0$ and all photopeaks to $\epsilon = 1$. With energies E and k in units of mc^2, this transformation is given by:

$$\epsilon(k) = E(2k+1)/k - 2k, \tag{3.7a}$$

$$\tilde{n}(\epsilon, k) = n(E,k)k/(2k+1). \tag{3.7b}$$

The transformed calibration spectra calculated for

ϵ values between −1.6 and +1.0 in steps of 0.01 are shown in Fig. 5. For each value of ϵ the interpolation between k values was performed by least-squares fitting a third-order polynomial function of k. From the resulting sets of coefficients the matrix elements r_{ij} were calculated by linear interpolation between neighboring ϵ values and by retransformation to the E scale.

The accuracy of the interpolation procedure was checked by recalculating the calibration spectra starting from line spectra. The agreement with the original spectra was better than 1 to 3% for the photopeak areas and for counts in channels around the Compton edges and at lower energies. Larger deviations (up to 5%) were observed only in the valley regions at the low-energy side of the peaks. This was mainly due to poorer counting statistics and small distortions of the calibration spectra due to pileup, but these low-intensity regions have minor influence on the response correction.

The accuracy of the determined response matrix R has finally been estimated to be 3% on the average, including the errors on the γ-emission rates of the calibration sources and on counting geometry (Sec. 2 C).

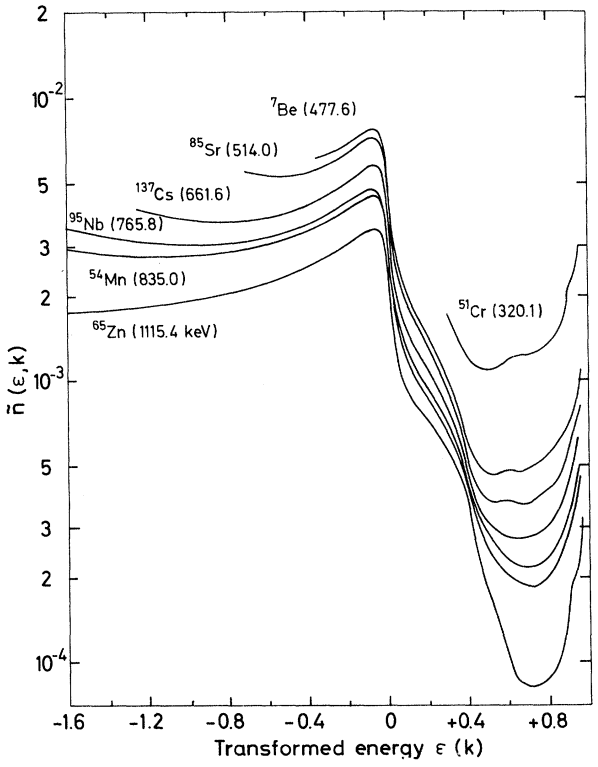

FIG. 5. Pulse-height spectra of calibration sources emitting single γ lines, transformed according to Eq. (3.7). The plotted portions of these spectra were used to construct the response matrix R of the Ge(Li) γ-ray spectrometer in the energy range from 320 keV to 1 MeV, except for elements near the diagonal of R.

For unfolding the measured pulse-height spectrum $n(E_i)$ in order to get $w(k_j)$, we applied an iterative method,[30] represented by ν iteration steps of the kind

$$w_i'^{(\nu)} = n_i - \sum_{j=1}^{m} (r'_{ij} - \delta_{ij}) w_j'^{(\nu-1)} \quad (i = 1, \ldots, m). \tag{3.8}$$

The prime indicates that, for this case, the response matrix has been normalized to unit peak areas[21] according to $r'_{ij} = r_{ij}/\epsilon_p(k_j)$, which leads to transformed spectra $w'_j = w_j \epsilon_p(k_j)$.

C. Results

1. IB Counting Rates

The IB spectrum $w_{\mathrm{IB}}^{\mathrm{th}}(k)$ deduced from Martin and Glauber's theory (Sec. 3 A) has been normalized to an energy interval of 1 keV and folded with the response matrix [Eq. (3.6)]. In Fig. 4 the resulting "theoretical" IB pulse-height spectrum $n_{\mathrm{IB}}^{\mathrm{th}}(E)$ per ground state EC decay of ^{51}Cr is compared with the experimental spectrum $n_{\mathrm{IB}}^{\mathrm{exp}}(E)$. Numerical results of integral rates $N_{\mathrm{IB}}(E_1 = \int_{E_1}^{Q_{\mathrm{EC}}} n_{\mathrm{IB}}(E)dE$ are listed in Table I for various low-energy limits E_1.

2. IB Intensities

Before unfolding the measured pulse-height spectrum $n_{\mathrm{IB}}^{\mathrm{exp}}(E)$ the number of channels was reduced by a factor 8, and the unfolding procedure [Eq. (3.8)] was tested by recalculating the theoretical spectrum $w_{\mathrm{IB}}^{\mathrm{th}}(k)$ starting from $n_{\mathrm{IB}}^{\mathrm{th}}(E)$. It was found that after six iteration steps the original $w_{\mathrm{IB}}^{\mathrm{th}}(k)$ was reproduced within 0.1% in all channels. In the inset of Fig. 4 the experimental IB spectrum calculated by six iterations from $n_{\mathrm{IB}}^{\mathrm{exp}}(E)$ is compared with $w_{\mathrm{IB}}^{\mathrm{th}}(k)$. The integral IB intensity obtained by integrating $w_{\mathrm{IB}}^{\mathrm{exp}}(k)$ over the energy range 348.1 keV $\leq k \leq Q_{\mathrm{EC}}$ is compared in Table II with corresponding theoretical values.

TABLE I. Measured IB counting rates per EC decay $N_{\mathrm{IB}}^{\mathrm{exp}}(E_1)$ compared with those calculated from the theoretical IB spectrum (see text).

E_1 (keV)	$N_{\mathrm{IB}}^{\mathrm{exp}}(E_1)$ Per 10^9 ground-state EC decays of ^{51}Cr	$N_{\mathrm{IB}}^{\mathrm{th}}(E_1)$
353.0	207 ± 8	200 ± 7
400.0	117 ± 7	112 ± 4
450.0	61.4 ± 5.0	56.9 ± 2.1
500.0	32.1 ± 4.0	28.0 ± 1.2
550.0	15.9 ± 3.5	12.2 ± 0.6
600.0	6.9 ± 2.5	4.8 ± 0.3

TABLE II. Comparison of measured IB intensities in ^{51}Cr with the predictions of theory.

	This work	Ref. 14	Ref. 18
Method	IB/γ	IB-γ coinc.	IB(circ. polar.)/γ
Decay	^{51}Cr(EC)^{51}V	^{51}Cr(EC)^{51}V*	
Transition energy (keV)	760 ± 15	429 ± 16	
	751.4 ± 0.9 [a]	431.3 ± 1.0 [a]	
Energy range (keV)	348.1–751.4	130–425	
IB/EC $\times 10^5$:			
Experiment	9.56 ± 0.60	7.2 ± 0.4	
Theory [b]: Martin and Glauber [c]	9.49 ± 0.05	5.56 ± 0.04	
Intemann	9.47 ± 0.05	5.66 ± 0.04	
Exp.-to-theor. IB yield:			
Martin and Glauber	1.01 ± 0.06	1.29 ± 0.08	0.67 ± 0.07
Intemann	1.01 ± 0.06	1.27 ± 0.08	

[a] These values were derived from Ref. 13.

[b] Transition energies from Ref. 13 were used. The errors on these values were used to calculate the quoted errors on the theoretical IB intensities.

[c] Calculated with 1s-IB shape factors from Eqs. (4.3) and (4.4) in Ref. 3.

3. *Error Analysis*

The errors on the IB counting rates $N_{IB}^{exp}(E_1)$ given in Table I are rms errors calculated, according to Eq. (2.5), from

(a) the standard errors on the corresponding rates per total counting rate $R_{IB}(E_1)$ (1.5% for $E_1 = 353.0$ keV to 30% for $E_1 = 600$ keV) that have been obtained by weighted linear fits [Eq. (2.4)] and represent the statistical counting errors of all 10 measurements, and

(b) the systematic errors on the γ branching ratio P_γ (2.0%), the average detection efficiency for ^{51}Cr γ rays ϵ_γ^0 (2.3%, as composed of the standard deviation of 1.8% from 10 results and 0.5% due to the γ-decay-rate calibration of the ^{51}Cr sources), and the energy interval per channel width ΔE (0.2%).

The errors given on the theoretical quantities $N_{IB}^{th}(E_1)$ correspond to the sum of the estimated error (3%) on the response matrix (Sec. 3B) and uncertainties of 0.5 to 1.7% that are induced on the predicted IB intensities for $k \geq E_1$ by the uncertainty on the value of 751.4 ± 0.9 keV, recommended for Q_{EC} of ^{51}Cr.[13]

The error on the measured IB intensity, given in Table II, is the error of 3.2% on the corresponding counting rate N_{IB}^{exp} ($E_1 = 348.1$ keV) plus 3% due to the response correction.

4. *Average IB Shape Function R_s*

An experimental result for the over-all shape function $R_s(Z, k)$ for s IB [Eq. (3.4)] was derived by dividing $w_{IB}^{exp}(k)$ by the Morrison-Schiff spectrum $w_{IB}^{CE}(k, k_{max}^{1s})$ [Eq. (3.3)]. The accuracy of the data was not sufficient for an establishment of the weak energy dependence of $R_s(Z, k)$, but its absolute value could be well determined: Averaging over the energy range 348.1 keV $\leq k \leq$ 602.4 keV has yielded $\langle R_s(\text{exp}) \rangle = 0.63 \pm 0.06$ (standard deviation of 20 values) as compared to the theoretical value $\langle R_s(\text{theor.}) \rangle = 0.634$.

5. *Transition Energy of ^{51}Cr*

A properly normalized Jauch plot[31] was constructed from $w_{IB}^{exp}(k)$ by using the relations of Eqs. (3.2) to (3.5), according to

$$F(k) \equiv [w_{IB}^{exp}(k)/(\alpha/\pi)kR_s(Z, k)]^{1/2} = (k_{max}^{1s} - k)/k_{max}^{1s} . \quad (3.9)$$

A linear least-squares fit to the data $F(k)$ in the energy range 348.1 keV $\leq k \leq$ 666.3 keV (Fig. 6) has yielded for k_{max}^{1s} a value of 754 ± 10 keV. Fitting the same data, but neglecting the predicted

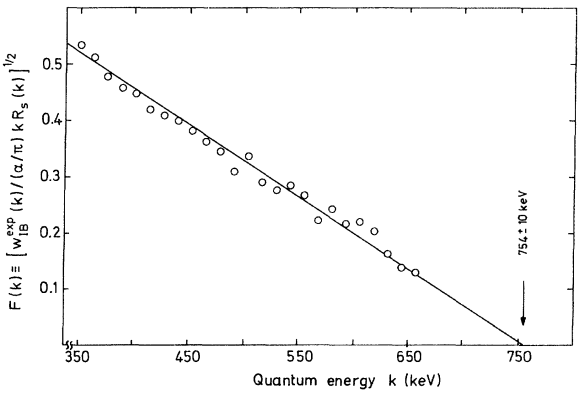

FIG. 6. Jauch plot of ^{51}Cr. The experimental data were calculated from $w_{IB}^{exp}(k)$ according to Eq. (3.9). The straight line fitted to these data has yielded for the end-point energy of the 1s-IB spectrum of ^{51}Cr values 754 ± 10 keV and 776 ± 30 keV, deduced from the intercept and the slope, respectively.

energy dependence of the shape factors by setting $R_{1s} = R_{2s} = 1$ in Eq. (3.4) has yielded $k^{1s}_{max} = 749 \pm 10$ keV. Since the predicted energy dependence of the shape factors has never been confirmed experimentally until now the difference of 5 keV with respect to the upper result is adopted as an additional systematic error, leading to the final result of $k^{1s}_{max} = 754 \pm 15$ keV. The transition energy of ^{51}Cr is consequently $Q_{EC} = 760 \pm 15$ keV. This value is in good agreement with 750 ± 6 keV [32] and 751 ± 3 keV,[33] obtained from the nuclear threshold reaction ^{51}V$(p, n)^{51}$Cr, as well as with the recommended value 751.4 ± 0.9.[13]

As seen from the right side of Eq. (3.9), the $1s$ end-point energy must also be represented by the negative inverse slope of a properly normalized Jauch plot. From the data $F(k)$ a value of 776 ± 30 keV has been derived in this way, in fair agreement with the upper result. Although this value is less accurate than that deduced in the usual way from the line's intercept with the k axis, this alternative method may be of some interest, e.g., for s-IB spectra of higher-Z EC nuclides, where the function $h(k)$ [Eq. (3.5)] introduces some uncertainty on $F(k)$ values except far below the IB end-point energy.

4. DISCUSSION

The present results confirm the prediction of the Martin-Glauber theory for radiative capture of $1s + 2s$ orbital electrons: Agreement within a few per cent was found for the shape of the IB spectrum as well as for the relative rate of radiative to ordinary capture. The measured $1s$-IB end-point energy comes into close agreement with accepted atomic mass differences.

The confirmation of the predicted rate of radiative to ordinary capture by the present experiment is consistent with the result of a $1s$-IB-KX coincidence experiment on the heavier nuclide ^{165}Er.[34] The present result is, however, in contradiction to recent experiments[14,18] on ^{51}Cr (results are included in Table II), and on the EC-decaying light nuclides ^{7}Be, ^{54}Mn, and ^{57}Co.[14-17] Although, with one exception,[18] these were IB-γ-coincidence experiments, performed similarly with NaI detectors in face-to-face geometry, the reported results are very contradictory.[14]

There are reasons to believe that the over-all accuracy achieved by these IB-γ-coincidence experiments has partly been overestimated. The measurement of IB-γ coincidences is complicated by the fact that both types of radiation, being different in intensity by about 10^{-4}, contribute to the same spectral range. Scattering between the crystals gives further complications, which might have caused the low IB rates obtained by Lancman and Lebowitz[15] (see Ref. 14). But it may be assumed that the latter effect cannot account for the difference of about a factor of 2 between the IB rates for ^{54}Mn and ^{57}Co, reported by Lancman and Lebowitz,[15] and those for ^{51}Cr and ^{54}Mn, given by Koonin and Persson.[14]

According to the theoretical calculations of Intemann,[6] the omission of higher-order terms in $Z\alpha$ in the Martin and Glauber theory tends to a slight underestimation of the $1s$-IB intensity and to a more pronounced overestimation of the $2s$-IB intensity. For ^{51}Cr, Intemann's calculations yield an increase of the $1s$-IB intensity in the energy range of the present experiment of about 3% compared to the Martin and Glauber result, but a decrease of the $2s$-IB component of about 23%. Both deficiencies in the Martin-Glauber theory nearly cancel in the calculation of the $1s + 2s$-IB spectrum, as can be seen from Table II.

ACKNOWLEDGMENTS

I am very much indebted to Professor Dr. A. H. W. Aten, Jr. and Dr. J. Spaepen, present and former director of the Central Bureau for Nuclear Measurements for their kind hospitality, to A. Spernol, who initiated and supported this work, and to Professor Dr. H. Vonach, Technische Universität München, for his continuous interest. The assistance of many members of the radionuclides group of the Central Bureau for Nuclear Measurements is gratefully acknowledged, especially B. Denecke for performing part of the Ge(Li) measurements, P. Klopf for improvement of the electronic equipment, W. van der Eyk and W. Zehner for the purification of the ^{51}Cr solution and for source preparation, R. Vaninbroukx and G. Grosse for the γ calibration of the sources, and G. Bortels for performing part of the extensive computer calculations. I am very grateful to Professor Dr. R. L. Intemann for providing me with the computer code of his theoretical calculations.

---

†This work has been supported by a European Community Research Grant.

*Part of a dissertation accepted and approved by the "Fakultät für Allgemeine Wissenschaften der Technischen Universität München," Munich, Germany, in partial fulfillment of the requirements for the degree of Dr. rer. nat.

[1] R. Morrison and L. I. Schiff, Phys. Rev. 58, 24 (1940).
[2] R. J. Glauber and P. C. Martin, Phys. Rev. 104, 158 (1956).

[3]P. C. Martin and R. J. Glauber, Phys. Rev. 109, 1307 (1958).
[4]B. A. Zon and L. P. Rapoport, Yad. Fiz. 7, 528 (1968) [transl.: Sov. J. Nucl. Phys. 7, 330 (1968)].
[5]B. A. Zon, Yad. Fiz. 13, 963 (1971) [transl.: Sov. J. Nucl. Phys. 13, 554 (1971)].
[6]R. L. Intemann, Phys. Rev. C 3, 1 (1971).
[7]R. E. Cutkosky, Phys. Rev. 107, 330 (1957).
[8]S. F. Timashev and V. A. Kaminskii, Zh. Eksp. Teor. Fiz. 38, 284 (1960) [transl.: Sov. Phys.-JETP 11, 206 (1960)].
[9]Y. Koh, O. Miyatake, and Y. Watanabe, Nucl. Phys. 32, 246 (1962).
[10]J. Zylicz, in *Proceedings of the International Conference on Electron Capture and Higher-Order Processes in Nuclear Decay, Debrecen, Hungary, 15–18 July, 1968,* edited by D. Berényi (Eötvös Lóránd Physical Society, Budapest, Hungary, 1968), Vol. 2, p. 123. See also Ref. 14.
[11]M. Mutterer, to be published.
[12]W. D. Brewer and D. A. Shirley, Phys. Rev. Lett. 20, 885 (1968).
[13]A. H. Wapstra and N. B. Gove, Nucl. Data A9, 267 (1971).
[14]S. E. Koonin and B. I. Persson, Phys. Rev. C 6, 1713 (1972).
[15]H. Lancman and J. M. Lebowitz, Phys. Rev. C 3, 465 (1971); Phys. Rev. 188, 1683 (1969); Phys. Rev. C 3, 188 (1971).
[16]I. Kádár, D. Berenyi, and B. Mysĺek, Nucl. Phys. A153, 383 (1970). The quoted theoretical value of 2.01×10^{-4} for the s-IB intensity per K capture in ^{54}Mn changes to 1.31×10^{-4} by adopting an energy of 540.1 keV (Ref. 13) for the EC transition from ^{54}Mn to the first excited state in ^{54}Cr.
[17]B. I. Persson and S. E. Koonin, Phys. Rev. C 5, 1443 (1972).
[18]J. C. Vanderleeden, F. Boehm, and E. D. Lipson, Phys. Rev. C 4, 2218 (1971).
[19]M. Mutterer, to be published.
[20]International Atomic Energy Agency Laboratory activities, Seventh Report, Technical Report Series No. 103, 1970 (unpublished), p. 22.
[21]C. Ribordy and O. Huber, Helv. Phys. Acta 43, 345 (1970).
[22]R. Vaninbroukx and G. Grossse, Int. J. Appl. Radiat. Isot. 17, 41 (1966).
[23]F. E. Butler, A. R. Boulogne, and E. A. Whitley, Health Phys. 12, 927 (1966).
[24]J. H. Williamson, Can. J. Phys. 46, 1845 (1968).
[25]E. De Roost and F. Lagoutine, to be published.
[26]$P_L/P_K = 0.103 \pm 0.002$: mean value of data given by G. Manduchi and G. Zannoni, Nuovo Cimento 27, 251 (1963); and W. Heuer and E. Huster, Z. Naturforsch. 19a, 517 (1964).
[27]L. N. Zyryanova and Yu. P. Suslov, Izv. Akad. Nauk SSSR Ser. Fiz. 33, 1693 (1969)[transl.: Bull. Acad. Sci. USSR Phys. Ser. 33, 1553 (1969)].
[28]H. Behrens and J. Jänecke, in *Landotl-Börnstein: Numerical Data and Functional Relationships in Science and Technology,* edited by H. Schopper (Springer, Berlin, 1969), New Series, Group I, Vol. 4.
[29]J. A. Bearden, Rev. Mod. Phys. 39, 78 (1967).
[30]G. E. Owen and H. Primakoff, Phys. Rev. 74, 1406 (1948).
[31]J. M. Jauch, Oak Ridge National Laboratory Report No. ORNL-1102, 1951 (unpublished); P. R. Bell, J. M. Jauch, and J. M. Cassidy, Science 15, 12 (1952).
[32]H. T. Richards, R. V. Smith, and P. C. Browne, Phys. Rev. 80, 524 (1950).
[33]C. R. Gossett and J. W. Butler, Phys. Rev. 113, 246 (1959).
[34]Z. Sujkowski, J. Jastrzebski, A. Zglinski, and J. Zylicz, in *Proceedings of the International Conference on the Role of Atomic Electrons in Nuclear Transformations, Warsaw, Poland, 24–28 September 1963* (Nuclear Energy Information Center, Warsaw, Poland, 1965), Vol. IV, p. 614.